Current Biology 22, 64–69, January 10, 2012 ©2012 Elsevier Ltd All rights reserved DOI 10.1016/j.cub.2011.11.040

Report

Cleavage Furrow Organization Requires PIP_2-Mediated Recruitment of Anillin

Jinghe Liu,[1,2] Gregory D. Fairn,[3] Derek F. Ceccarelli,[4] Frank Sicheri,[1,2,4] and Andrew Wilde[1,2,*]

[1]Department of Molecular Genetics

[2]Department of Biochemistry

University of Toronto, Toronto, ON M5S 1A8, Canada

[3]Program in Cell Biology, Hospital for Sick Children, Toronto, ON M5S 1X8, Canada

[4]Samuel Lunenfeld Research Institute, Mount Sinai Hospital, Toronto, ON M5S 1X5, Canada

Summary

Cell division is achieved by a plasma membrane furrow that must ingress between the segregating chromosomes during anaphase [1–3]. The force that drives furrow ingression is generated by the actomyosin cytoskeleton, which is linked to the membrane by an as yet undefined molecular mechanism. A key component of the membrane furrow is anillin. Upon targeting to the furrow through its pleckstrin homology (PH) domain, anillin acts as a scaffold linking the actomyosin and septin cytoskeletons to maintain furrow stability (reviewed in [4, 5]). We report that the PH domain of anillin interacts with phosphatidylinositol phosphate lipids (PIPs), including $PI(4,5)P_2$, which is enriched in the furrow. Reduction of cellular $PI(4,5)P_2$ or mutations in the PH domain of anillin that specifically disrupt the interaction with $PI(4,5)P_2$, interfere with the localization of anillin to the furrow. Reduced expression of anillin disrupts symmetric furrow ingression that can be restored by targeting ectopically expressed anillin to the furrow using an alternate $PI(4,5)P_2$ binding module, a condition where the septin cytoskeleton is not recruited to the plasma membrane. These data demonstrate that the anillin PH domain has two functions: targeting anillin to the furrow by binding to $PI(4,5)P_2$ to maintain furrow organization and recruiting septins to the furrow.

Results and Discussion

Anillin Binds to PIPs

The C-terminal portion of anillin is required for its targeting to the cleavage furrow [6, 7], but the mechanism of targeting has not been defined. This region of anillin contains a pleckstrin homology (PH) domain and an adjacent region conserved across anillin species, the anillin homology (AH) domain (Figure 1A). In *Drosophila melanogaster*, a group of maternal-effect lethal mutations that disrupt cellularization and the hatching of embryos was discovered to be a series of point mutations in the PH domain of anillin [8]. These defects stem from a reduced stability of the pseudocleavage furrow that led to a failure of the furrows to enclose the nuclei to form individual cells. Furthermore, the mutant anillins were recruited less efficiently to the furrow and there was a progressive loss of the mutant anillins at the ingressing furrow canals, suggesting that the mutants have a reduced ability to interact with the membrane. We tested two of the mutants in HeLa cells, T991I, T, and G998E, G (equivalent to *D. melanogaster* T1076I, G1083E, respectively; [8]) and found that both GFP-tagged proteins failed to be targeted to the cleavage furrow (see Figures S1B and S1C available online), suggesting that the PH domain is involved in targeting anillin to the cleavage furrow.

The C terminus of anillin binds to many factors, including RhoA and septins [5]. However, we found that the T and G mutations in the PH domain did not disrupt anillin binding to RhoA-GTP or septins in in vitro binding assays (Figures 1B and 1C), suggesting that the failure of the mutant anillins to localize to the cleavage furrow was independent of RhoA and septins.

In the PH domain, the T mutation lies in the β1 strand, whereas the G mutation lies within the β1 and β2 connector, a region in other PH domains associated with PIP binding [9]. Therefore, the mutants may fail to localize to the furrow because of an inability of the PH domain to interact with PIPs. To test this model, we used a fluorescence polarization assay [10] to determine the dissociation constant for anillin binding to different phosphoinositide (PI) ligands. The human AH-PH (hAH-PH) region of anillin could not be concentrated sufficiently to allow the determination of dissociation constants. In contrast, *D. melanogaster* AH-PH (dAH-PH), amino acids 815–1,201 [11], was stable at high concentrations. dAH-PH preferentially bound to $PI(3,4,5)P_3$, $PI(4,5)P_2$, $PI(3,4)P_2$, and PI(5)P compared to other PIPs that bound weakly with dissociation constants greater than 150 μM (Figure S1D; Table 1). To further confirm these interactions, we assayed the ability of AH-PH to comigrate with liposomes containing different PIPs on sucrose flotation gradients (Figures 1E and 1F). Proteins and liposomes were mixed and layered underneath a sucrose gradient. After centrifugation, liposome associated proteins are in the upper part of the sucrose gradient, the supernatant fraction (S), whereas proteins that did not bind to liposomes are in the lower fraction, the pellet (P). dAH-PH (Figure 1E; Figure S1F) and hAH-PH (Figure 1F; Figure S1G) comigrate with liposomes containing $PI(3,4,5)P_3$ and $PI(4,5)P_2$, demonstrating a conserved interaction with these lipids. However, binding to PI(5)P and $PI(3,4)P_2$ was not conserved. The reason for this difference between the assays is unclear, but perhaps when presented in the context of a liposome rather than just the lipid head group, the AH-PH domain exhibits different binding characteristics. These data suggest a conserved binding activity of AH-PH domains of anillin for $PI(3,4,5)P_3$ and $PI(4,5)P_2$.

Mutations in the PH Domain Reduce PIP Binding

As the T and G mutations disrupt anillin targeting to the cleavage furrow (Figures S1B and S1C), we examined the interaction of the mutants with PIPs. For dAH-PH, the T and G mutations showed a 2- to 3-fold reduction in binding to $PI(3,4,5)P_3$ but a 10- to 20-fold reduction in binding to $PI(4,5)P_2$, $PI(3,4)P_2$, and PI(5)P (Table 1). Likewise, the T and G mutants of hAH-PH exhibited similar qualitative differences in binding to these lipids (Figure 1G). Furthermore, the T and G mutants in both dAH-PH and hAH-PH exhibited

*Correspondence: andrew.wilde@utoronto.ca

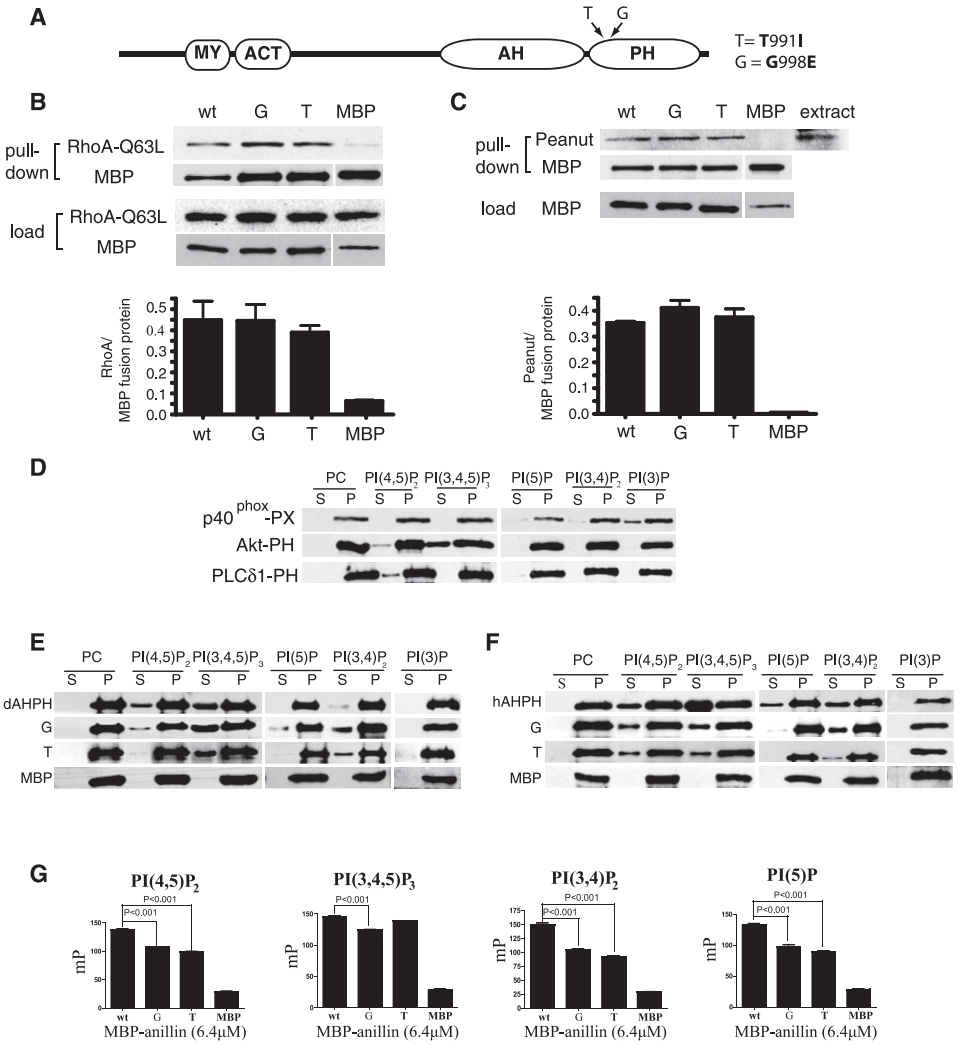

Figure 1. AH-PH Domain of Anillin Binds to PIPs

(A) A schematic diagram of the domain organization of anillin. MY, myosin binding domain; ACT, actin binding domain; AH, anillin homology domain; PH, pleckstrin homology domain.

(B) The anillin AH-PH domain interacts with RhoA-GTP. AH-PH domain (fused to maltose-binding protein [MBP]) binds to the activated allele of RhoA, RhoA-Q63L (fused to GST). The upper panel shows representative blot of pull-downs, and the lower panel shows quantitation of band intensities of three repeats of the pull-down experiment. Error bars are ± SEM.

(C) MBP-AH-PH incubated with *D. melanogaster* embryo extract then recovered using amylose beads. Copurifying *D. melanogaster* septin Peanut was identified by western blotting. The upper panel shows representative blot, and the lower panel shows quantitation of band intensities of three repeats of the pull-down experiment. Error bars are ± SEM.

(D) Control PIP liposome binding assays. GST-p40^{phox}-PX binds to PI(3)P, MBP-Akt-PH domain binds to PI(3,4,5)P_3, and MBP-PLCδ1-PH domain binds to PI(4,5)P_2. S, liposomes bound fraction; P, unbound fraction. Representative blot with quantitation is shown in Figure S1.

(E) MBP dAH-PH domain liposome binding assay; wt, wild-type; T, T1076I; G, G1083E. Representative blot with quantitation is shown in Figure S1.

(F) MBP-hAHPH liposomes binding assay; wt, wild-type; T, T991I; G, G998E G. Representative blot with quantitation is shown in Figure S1.

(G) Binding of MBP-hAH-PH to BODIPY-labeled phosphoinositides (mP, millipolarization units). Error bars are ± SEM.

reduced interactions with PI(4,5)P_2 containing liposomes (Figures 1E and 1F; Figures S1F and S1G). In contrast, only the hAH-PH domain had a reduced interaction with PI(3,4,5)P_3. Again the binding of hAH-PH and dAH-PH to PI(3,4)P_2 and PI(5)P was not consistent across species. How the mutations within the PH domain affect PIP binding is unclear. Based on the crystal structure of the human anillin PH domain [12], the G998E would introduce a negative charge into a putative PIP binding pocket, but the T991I mutation, which does not lie in the pocket, may be expected to have an indirect effect.

Taken together, these data demonstrate that the anillin-PI(4,5)P_2 binding is conserved across phyla and binding assays. Because depletion of PI(4,5)P_2 levels disrupts cytokinesis [13–15], our observation that anillin mutations disrupt PI(4,5)P_2 binding and furrow targeting provide a possible mechanism for how anillin is targeted to the cleavage furrow.

PI(4,5)P_2 Is Required for Anillin Targeting to the Cleavage Furrow

PI(4,5)P_2 accumulates at the cleavage furrow and is required for successful completion of cytokinesis [13, 14] (Figure 2). In contrast, other PIPs, PI(3,4,5)P_3 and PI(3)P and phosphatidylserine (PS) localize throughout the plasma membrane but do not become enriched at the cleavage furrow (Figure 2).

Table 1. Dissociation Constants of *Drosophila* Anillin AHPH Domain Constructs for PIPs ± SEM

MBP Fusion Protein Constructs	$PI(3,4,5)P_3$	$PI(4,5)P_2$	$PI(3,4)P_2$	PI(5)P	PI(3)P	PI(4)P	$PI(3,5)P_2$	Inositol
WT	4. 5 ± 0.1	5.3 ± 0.3	7.8 ± 0.4	7.8 ± 0.7	29.61 ± 4.78	38.50 ± 5.88	41.58 ± 9.00	155.6 ± 70.9
G1083E	10.2 ± 0.8	58.8 ± 19.2	97.1 ± 44.1	134.4 ± 56.27	>150	>150	>150	>150
T1076I	17.3 ± 1.59	56.3 ± 7.1	104.4 ± 23.4	60.5 ± 7.5	nd	nd	nd	>150
PLCδ1 PH	0.14 ± 0.008	0.02 ± 0.003	nd	nd	16.58 ± 1.54	nd	nd	135.2 ± 33.56
Akt PH	0.15 ± 0.007	8.14 ± 0.33	nd	nd	nd	nd	nd	11.37 ± 0.64
$p40^{phox}$ PX	8.05 ± 0.46	43.55 ± 3.92	nd	nd	1.15 ± 0.06	nd	nd	53.52 ± 4.48
MBP	>150	>150	nd	nd	nd	>150	nd	169.4 ± 103.9

The following abbreviations are used: maltose-binding protein, MBP; wild-type, WT; nd, not determined.

To address which PIPs may be involved in targeting anillin to the furrow in vivo, we disrupted the production of different PIPs within the cell. The PI3 kinase inhibitor wortmannin [16] inhibits phosphorylation of the 3 position on the inositol ring, but did not prevent targeting of anillin or a $PI(4,5)P_2$ biosensor to the cleavage furrow. In contrast, plasma membrane targeting of a $PI(3,4,5)P_3$ biosensor was disrupted under these conditions (Figure 2B). These data suggest that $PI(3,4,5)P_3$, $PI(3,4)P_2$, and PI(3)P do not play a prominent role in recruiting anillin to the cleavage furrow.

To assess the involvement of $PI(4,5)P_2$ in anillin targeting, we reduced cellular levels of $PI(4,5)P_2$ by expressing a membrane-targeted form of the $PI(4,5)P_2$-specific PI5P phosphatase domain of synaptojanin 2 (Sj2) [17–19]. In cells expressing Sj2, anillin and the $PI(4,5)P_2$ biosensor were diffuse throughout the plasma membrane rather than localizing to the cleavage furrow (Figure 2C). These data suggest that a PIP with a phosphate at the 5 position is required for anillin recruitment to the furrow, the best candidate being $PI(4,5)P_2$. Consistent with this model, a recent study found that the redistribution of $PI(4,5)P_2$ to large cytoplasmic vacuoles resulted in a concomitant redistribution of anillin to these vesicles from the plasma membrane during cytokinesis [15]. Although anillin has a lower affinity for $PI(4,5)P_2$ than other $PI(4,5)P_2$-specific binding PH domains, consideration must be given to the abundance of the different lipids. $PI(4,5)P_2$ is 25-fold more abundant than PI(5)P, and 500-fold more abundant than $PI(3,4)P_2$ [9], suggesting that in vivo $PI(4,5)P_2$ is the most relevant ligand for the anillin PH domain and is involved in the enrichment of anillin at the cleavage furrow. Additionally, other factors may also influence anillin binding to PIPs in vivo. Multimerization of anillin, as the *S. pombe* homolog Mid1p [20], could increase its avidity for the $PI(4,5)P_2$, a mechanism utilized by dynamin [21]. Alternatively, $PI(4,5)P_2$ binding to anillin could affect anillin's interaction with other binding partners, thereby regulating anillin activity during cytokinesis.

Anillin-PIP Interaction Is Required for Cytokinesis and Actin Enrichment at the Furrow

To determine the role of anillin binding to $PI(4,5)P_2$ in cytokinesis, we carried out small interfering RNA (siRNA) rescue experiments where endogenous anillin was depleted by siRNA in cells expressing siRNA-resistant variants of anillin (Figure S2). Depletion of anillin caused an increase in the percentage of binucleate cells, a phenotype reversed upon expression of wild-type siRNA resistant anillin. However, anillin containing the T and G mutations could not rescue cytokinesis (Figures S2B and S2C), suggesting that cytokinesis requires anillin to interact with $PI(4,5)P_2$.

To determine whether the only role of the PH domain is to bind $PI(4,5)P_2$, we created a chimeric anillin where the PH domain was replaced by the $PI(4,5)P_2$ binding PH domain of phospholipase C-δ1, PLCδ1. The chimeric anillin, anillin-ΔPH + PLCδ1-PH, restored anillin localization (Figure 3A), whereas anillin ΔPH failed to localize to the furrow (Figure S1). However, in anillin-depleted cells expressing the chimera, cytokinesis could not be completed. Instead the binucleate phenotype persisted (Figure 3B), suggesting that the anillin PH domain is required for more than interacting with PIPs. The chimera localized to ingressing furrows (Figure 3A), suggesting the PH domain's additional role is at a later stage of cytokinesis.

To determine the additional function of the anillin PH domain, we analyzed the effect of chimera expression on known anillin interacting partners. Actin is normally enriched in the furrow, compared to the pole (13.74 ± 2.71-fold, Figure 3C; Figure S3A). However, depletion of anillin caused a redistribution of actin throughout the cortex of the cell (Figure 3C; Figure S3A) [7]. Expression of GFP-anillin or the chimera in anillin-depleted cells rescued actin recruitment to the furrow (15.95 ± 3.31- and 15.45 ± 4.90-fold enrichment, respectively; Figure 3C; Figure S3A).

The Anillin-PIP Interaction Is Required for Correct Furrow Ingression

In dividing wild-type cells, symmetrical furrow ingression occurs in the middle of the cell. In contrast, in anillin-depleted cells, furrow ingression did not stabilize in the center of the cell [7, 22–24] and ingression was asymmetric. We analyzed this further in live cells using RFP-Liveact [25] as a reporter for the actin cytoskeleton (Figures 3D and 3E; Figure S4). To quantify these observations, we generated two indices (Figure 3E). The symmetry index measured the ratio of the depth of furrow ingression on one side of the cell compared to the other side of the cell. An index of 1.00 indicates that the cleavage furrow ingresses equally and symmetrically, and indices above 1.00 indicate asymmetric furrow ingression. The stabilization index measures the ratio of the distance of the cleavage furrow from one pole of the cell to the other. An index of 1.00 indicates a centrally maintained furrow and indices greater than 1.00 indicate ingression away from the cell center.

Mock-treated cells had an ingression index of 1.11 ± 0.03 and a stabilization index of 1.06 ± 0.02 (Figure 3F). In contrast, depleting anillin resulted in an ingression index of 2.5 ± 0.24 and a stabilization index of 1.32 ± 0.1 (Figure 3F), indicating asymmetric furrow ingression that was not stabilized in the cell center. Expression of GFP-anillin rescued ingression symmetry (ingression index 1.09 ± 0.02) and furrow stabilization at the cell center (stabilization index 1.05 ± 0.01). Likewise, expression of the chimera rescued ingression symmetry (ingression index 1.1 ± 0.03) and almost completely rescued centralized furrow stabilization (stabilization index 1.1 ± 0.02)

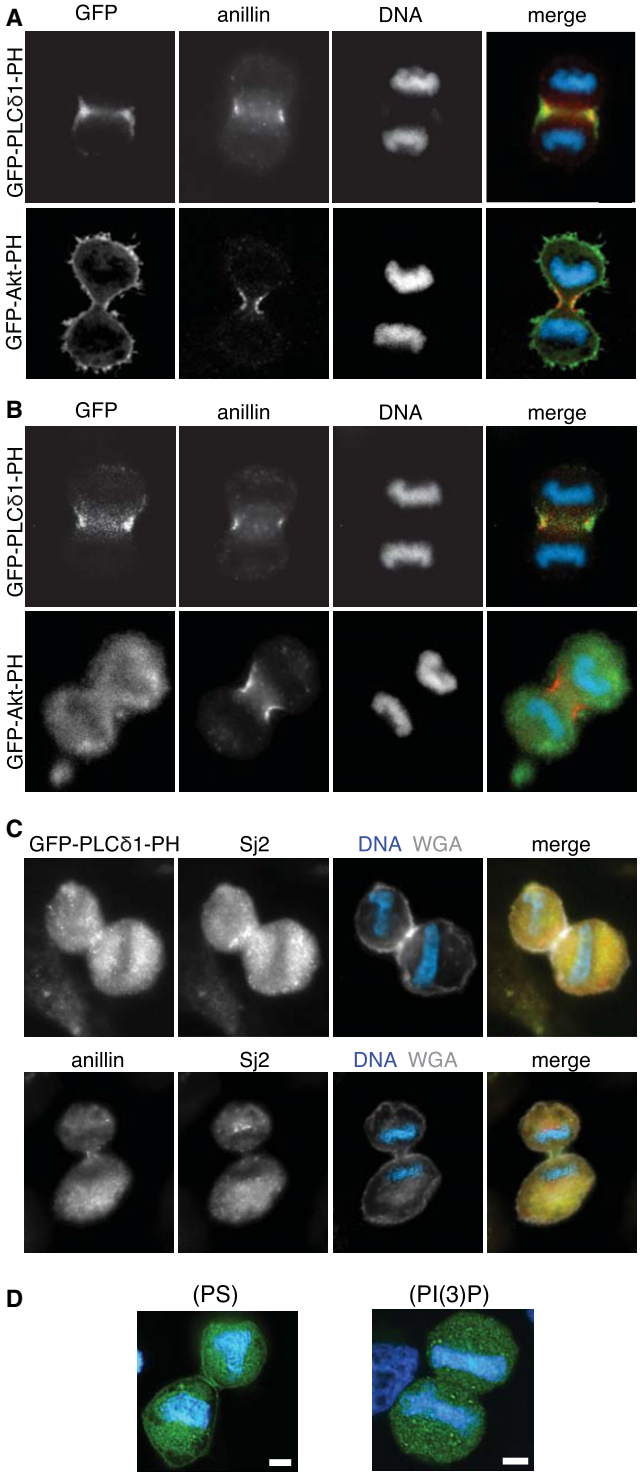

Figure 2. Anillin Colocalizes with and Is Dependent upon PI(4,5)P_2 for Localization to the Cleavage Furrow

(A) HeLa cells expressing GFP-PLCδ1-PH or GFP-Akt-PH costained with anillin.

(B) HeLa cells expressing GFP-PLCδ1-PH or GFP-Akt-PH were treated with 100 nM wortmannin, fixed, and stained for anillin.

(C) HeLa cells were transfected and GFP-PLCδ1-PH and myc tagged Sj2 (upper panels) or just myc tagged Sj2 (lower panels). Prior to fixation, cells were incubated with wheat germ agglutinin (WGA) to mark the plasma membrane, shown as gray in the merged micrographs.

(D) HeLa cells expressing GFP-Lact2-C2 and GFP-2 × FYVE biosensors for PS and PI(3)P, respectively.

(Figure 3F). To determine the role of PI(4,5)P_2 in these processes, we depleted PI(4,5)P_2 by expressing Sj2. Sj2 expression increased the ingression index (1.92 ± 0.15) and the stabilization index (1.28 ± 0.02) indicating that depletion of cellular levels of PI(4,5)P_2 causes similar effects on cleavage furrow ingression as depletion of anillin.

PIP and Septin Binding Are Functions of the Anillin PH Domain

Next, we examined the septins because the septin interacting domain lies in the C terminus of anillin [6]. Depletion of anillin caused a redistribution of septins 2, 9, and 11 from the furrow to the poles of the cell (Figure 3C; Figures S3B–S3D), a phenotype rescued by expression of GFP-anillin (Figure 3C; Figures S3B–S3D). In contrast, the chimera did not rescue septin-targeting to the furrow in anillin-depleted cells (Figure 3C; Figures S3B–S3D). These data suggest two functions for the PH domain: binding to PI(4,5)P_2 for furrow targeting and recruitment of the septin cytoskeleton to the furrow.

Our findings demonstrate at least two functions for the anillin PH domain: targeting anillin to the furrow through binding to PI(4,5)P_2 and recruitment of the septin cytoskeleton to the furrow. The PI(4,5)P_2 binding is required for targeting anillin to the furrow early in cytokinesis and facilitates the enrichment of actin at the furrow. Because the anillin chimera facilitates actin recruitment to the furrow in the absence of endogenous anillin, this suggests that actin recruitment can be independent of septin recruitment to the furrow. During this early phase of cytokinesis, the anillin-PI(4,5)P_2 interaction maintains the correct cortical tension to prevent the furrow sliding in the plane of the membrane, which anillin is necessary for [24]. In addition, in HeLa cells, anillin-PI(4,5)P_2 interaction maintains the equal application for the force generated by the cytokinetic ring allowing symmetrically ingression of the furrow. It is not clear why in HeLa cells anillin should be required to maintain furrow symmetry but in *Caenorhabditis elegans* embryos should be required to break symmetry [26]. These anillin functions are independent of septin recruitment to the furrow because the anillin chimera facilitates these functions in the absence of septins at the furrow. However, septin depletion causes similar effects on furrow stability as anillin depletion [27]. Therefore, in a wild-type cell, anillin and septins may function in complimentary pathways, perhaps through different downstream effectors, to maintain furrow stability. With the increasing number of anillin-interacting partners it will be important to determine the interrelationship of these interactions and how they regulate cytokinesis.

Experimental Procedures

A detailed description of the experimental procedure used in this study can be found in the Supplemental Information.

Supplemental Information

Supplemental Material includes four figures, one table, and Supplemental Experimental Procedures and can be found online at doi:10.1016/j.cub.2011.11.040.

Acknowledgments

We thank J. Brill and B. Lavoie for discussion and comments on the manuscript; W. Trimble for the Septin 2, 9, and 11 antibodies; C. McCulloch for RFP-Lifeact; and S. Grinstein for the GFP reporters, the Sj2-CAAX, and consultation on the preparation of liposomes. This work was supported by grants from the Canadian Cancer Society (700741) to A.W. and a grant

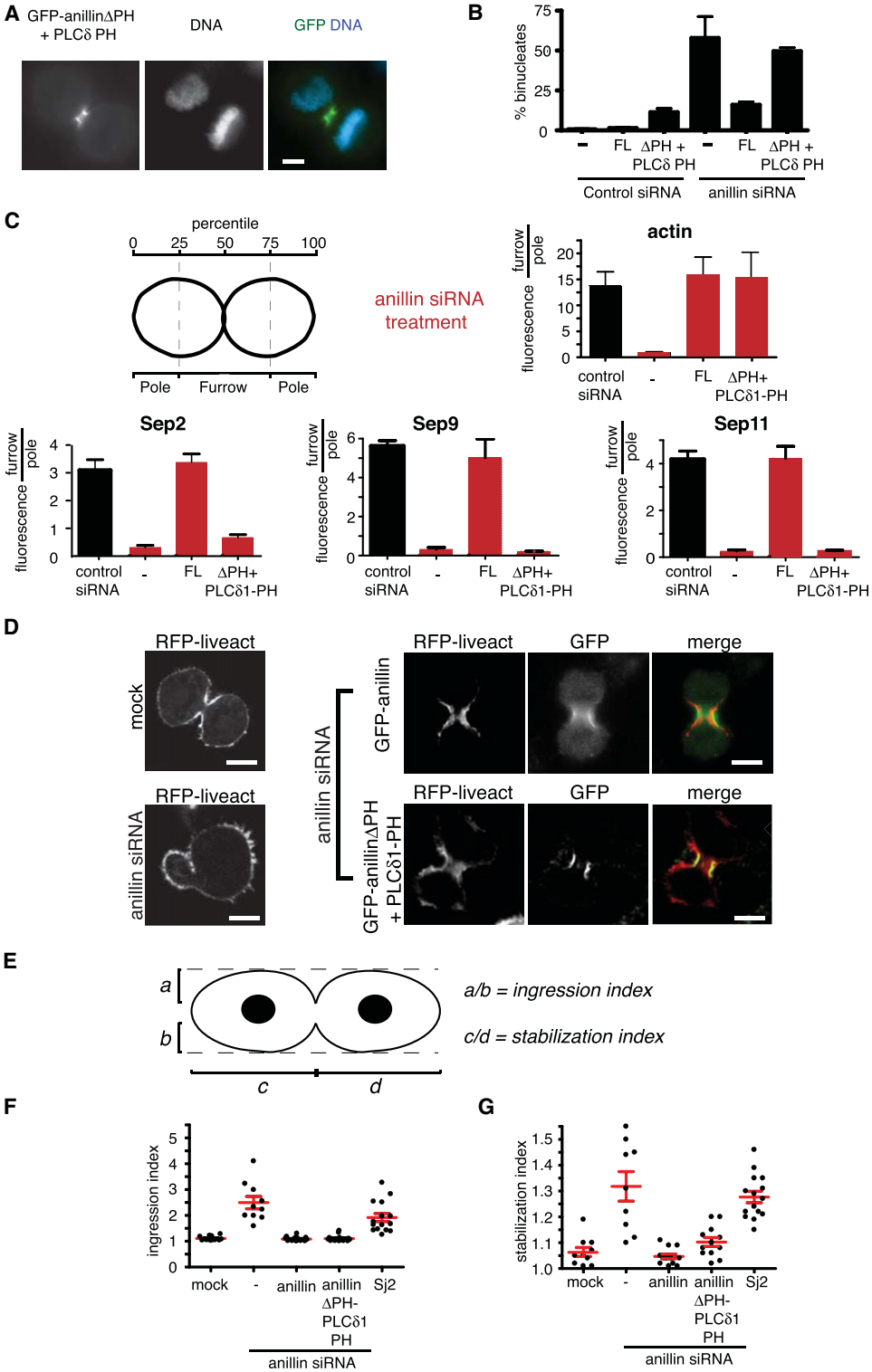

Figure 3. PIP and Septin Binding Are Functions of the Anillin PH Domain

The anillin PH domain has two functions: PI(4,5)P_2 binding that is required for stable symmetrical furrow ingression and septin binding that is required for the recruitment septin cytoskeleton to the furrow.

(A) GFP-ΔPH-anillin + PLCδ PH expressed in HeLa cells.

(B) The number of binucleate cells in anillin-depleted HeLa cells (–) expressing siRNA resistant GFP-anillin (FL) or GFP-ΔPH-anillin + PLCδ PH (ΔPH + PLCδ PH). Error bars indicate ± SEM.

(C) Distribution of actin and septins 2, 9, and 11 at the pole relative to the furrow in the presence and absence of wild-type anillin or anillin ΔPH + PLCδ1. The cartoon outlines how the regions of the cells were defined in which the fluorescence intensity of phalloidin (to detect actin) or anti-septin antibodies were measured. Red bars indicate cells treated with anillin siRNA. Error bars indicate ± SEM. Representative micrographs of actin and septins 2, 9, and 11 are shown in Figure S3.

from the Canadian Institute of Health Research (MOP 36399) to F.S. G.D.F. holds a postdoctoral fellowship from Canadian Institutes of Health Research, and A.W. holds a Canada Research Chair.

Received: July 18, 2011
Revised: October 19, 2011
Accepted: November 21, 2011
Published online: December 22, 2011

References

1. Eggert, U.S., Mitchison, T.J., and Field, C.M. (2006). Animal cytokinesis: from parts list to mechanisms. Annu. Rev. Biochem. *75*, 543–566.
2. Barr, F.A., and Gruneberg, U. (2007). Cytokinesis: placing and making the final cut. Cell *131*, 847–860.
3. Glotzer, M. (2005). The molecular requirements for cytokinesis. Science *307*, 1735–1739.
4. D'Avino, P.P. (2009). How to scaffold the contractile ring for a safe cytokinesis - lessons from Anillin-related proteins. J. Cell Sci. *122*, 1071–1079.
5. Piekny, A.J., and Maddox, A.S. (2010). The myriad roles of Anillin during cytokinesis. Semin. Cell Dev. Biol. *21*, 881–891.
6. Oegema, K., Savoian, M.S., Mitchison, T.J., and Field, C.M. (2000). Functional analysis of a human homologue of the *Drosophila* actin binding protein anillin suggests a role in cytokinesis. J. Cell Biol. *150*, 539–552.
7. Piekny, A.J., and Glotzer, M. (2008). Anillin is a scaffold protein that links RhoA, actin, and myosin during cytokinesis. Curr. Biol. *18*, 30–36.
8. Field, C.M., Coughlin, M., Doberstein, S., Marty, T., and Sullivan, W. (2005). Characterization of anillin mutants reveals essential roles in septin localization and plasma membrane integrity. Development *132*, 2849–2860.
9. Lemmon, M.A. (2008). Membrane recognition by phospholipid-binding domains. Nat. Rev. Mol. Cell Biol. *9*, 99–111.
10. Ceccarelli, D.F.J., Blasutig, I.M., Goudreault, M., Li, Z., Ruston, J., Pawson, T., and Sicheri, F. (2007). Non-canonical interaction of phosphoinositides with pleckstrin homology domains of Tiam1 and ArhGAP9. J. Biol. Chem. *282*, 13864–13874.
11. Silverman-Gavrila, R.V., Hales, K.G., and Wilde, A. (2008). Anillin-mediated targeting of peanut to pseudocleavage furrows is regulated by the GTPase Ran. Mol. Biol. Cell *19*, 3735–3744.
12. Vollmar, M., Wang, J., Krojer, T., Elkins, J., Filippakopoulos, P., Ugochukwu, E., Cocking, R., Vondelft, F., Bouta, C., Arrowsmith, C.H., et al. (2011). Human Actin-binding protein anillin (PH domain) (http://www.thesgc.org/structures/details?pdbid=2Y7B/).
13. Wong, R., Hadjiyanni, I., Wei, H.C., Polevoy, G., McBride, R., Sem, K.P., and Brill, J.A. (2005). PIP2 hydrolysis and calcium release are required for cytokinesis in *Drosophila* spermatocytes. Curr. Biol. *15*, 1401–1406.
14. Field, S.J., Madson, N., Kerr, M.L., Galbraith, K.A., Kennedy, C.E., Tahiliani, M., Wilkins, A., and Cantley, L.C. (2005). PtdIns(4,5)P2 functions at the cleavage furrow during cytokinesis. Curr. Biol. *15*, 1407–1412.
15. Ben El Kadhi, K., Roubinet, C., Solinet, S., Emery, G., and Carréno, S. (2011). The inositol 5-phosphatase dOCRL controls PI(4,5)P2 homeostasis and is necessary for cytokinesis. Curr. Biol. *21*, 1074–1079.
16. Okada, T., Kawano, Y., Sakakibara, T., Hazeki, O., and Ui, M. (1994). Essential role of phosphatidylinositol 3-kinase in insulin-induced glucose transport and antilipolysis in rat adipocytes. Studies with a selective inhibitor wortmannin. J. Biol. Chem. *269*, 3568–3573.
17. Malecz, N., McCabe, P.C., Spaargaren, C., Qiu, R.-G., Chuang, Y.-Y., and Symons, M. (2000). Synaptojanin 2, a novel Rac1 effector that regulates clathrin-mediated endocytosis. Curr. Biol. *10*, 1383–1386.
18. Mason, D., Mallo, G.V., Terebiznik, M.R., Payrastre, B., Finlay, B.B., Brumell, J.H., Rameh, L., and Grinstein, S. (2007). Alteration of epithelial structure and function associated with PtdIns(4,5)P2 degradation by a bacterial phosphatase. J. Gen. Physiol. *129*, 267–283.
19. Sakisaka, T., Itoh, T., Miura, K., and Takenawa, T. (1997). Phosphatidylinositol 4,5-bisphosphate phosphatase regulates the rearrangement of actin filaments. Mol. Cell. Biol. *17*, 3841–3849.
20. Celton-Morizur, S., Bordes, N., Fraisier, V., Tran, P.T., and Paoletti, A. (2004). C-terminal anchoring of mid1p to membranes stabilizes cytokinetic ring position in early mitosis in fission yeast. Mol. Cell. Biol. *24*, 10621–10635.
21. Klein, D.E., Lee, A., Frank, D.W., Marks, M.S., and Lemmon, M.A. (1998). The pleckstrin homology domains of dynamin isoforms require oligomerization for high affinity phosphoinositide binding. J. Biol. Chem. *273*, 27725–27733.
22. Straight, A.F., Field, C.M., and Mitchison, T.J. (2005). Anillin binds nonmuscle myosin II and regulates the contractile ring. Mol. Biol. Cell *16*, 193–201.
23. Zhao, W.M., and Fang, G. (2005). Anillin is a substrate of anaphase-promoting complex/cyclosome (APC/C) that controls spatial contractility of myosin during late cytokinesis. J. Biol. Chem. *280*, 33516–33524.
24. Sedzinski, J., Biro, M., Oswald, A., Tinevez, J.Y., Salbreux, G., and Paluch, E. (2011). Polar actomyosin contractility destabilizes the position of the cytokinetic furrow. Nature *476*, 462–466.
25. Riedl, J., Crevenna, A.H., Kessenbrock, K., Yu, J.H., Neukirchen, D., Bista, M., Bradke, F., Jenne, D., Holak, T.A., Werb, Z., et al. (2008). Lifeact: a versatile marker to visualize F-actin. Nat. Methods *5*, 605–607.
26. Maddox, A.S., Lewellyn, L., Desai, A., and Oegema, K. (2007). Anillin and the septins promote asymmetric ingression of the cytokinetic furrow. Dev. Cell *12*, 827–835.
27. Estey, M.P., Di Ciano-Oliveira, C., Froese, C.D., Bejide, M.T., and Trimble, W.S. (2010). Distinct roles of septins in cytokinesis: SEPT9 mediates midbody abscission. J. Cell Biol. *191*, 741–749.

(D) Furrow organization in anillin-depleted cells. Images taken from time-lapse series (Figure S4) of cells expressing Lifeact in the presence of absence of different anillin constructs.
(E) Cartoon outlining how the different furrow indices in (F) were calculated, where $a > b$ (ingression index) and $c > d$ (stabilization index).
(F) The ingression index in different conditions that measures the degree of symmetrical ingression.
(G) The stabilization index in different conditions that measures the position of stabilized furrow ingression relative to the long axis of the dividing cell.
Error bars are ± SEM.